Introduction

In regions characterized by complex subsurface structure, wave-equation depth migration is a powerful tool for accurately imaging the earth's interior. However, the quality of the final image greatly depends on the quality of the velocity model, thus constructing accurate velocity is essential for imaging.

One commonly used velocity estimation technique is migration velocity analysis (MVA). The input for such a technique is the migrated image obtained using an approximation of the velocity model. Velocity update is performed by adjusting the velocity model to optimize certain properties of the images, e.g. by using focusing or semblance analysis.

There are many practical possibilities to design a MVA technique. Owing to the challenge of velocity determination in complex subsurface region, wavefield-based MVA techniques which use band-limited wavefields as the information carrier to connect input image to the output velocity model draw more and more interests in recent years (Woodward, 1992; Pratt, 1999; Sirgue and Pratt, 2004). Wavefield-based MVA methods are capable of handling complicated wave propagation phenomena, which always happen in complex subsurface area, thus they are more robust and consistent with the wavefield-based migration techniques used in such regions. In this paper, our focus is on the wavefield-based migration velocity analysis method known as wave-equation MVA (Sava and Biondi, 2004a; Albertin et al., 2006).

For the implementation of WEMVA, one important component is the construction of an image perturbation which is linked linearly to a slowness perturbation (Sava and Biondi, 2004b). For the construction of image perturbation, the most common approach is to compare a reference image with an improved version of it. The image-comparison approach has at least two drawbacks. First, the improved version of the image is always obtained by re-migration with one or more models, which is computationally expensive. Second, if the reference image is incorrectly constructed, the difference between two images can exceed the small perturbation assumption, which leads to cycle skipping, as is the case for waveform-inversion in the data domain. An alternative to this approach, discussed in Sava (2003), uses prestack Stolt migration to construct a linearized image perturbation. This alternative approach avoids the cycle skipping problem, but suffers from the approximation embedded in the underlying Stolt migration.

Focusing analysis information can be extracted from time-lag extended images (Sava and Fomel, 2006). The focusing error is measured along the time-lag axis and quantified as the departure of the focusing time-lag from zero. Higginbotham and Brown (2008) propose a method to convert this focusing error into velocity updates for the background model using vertical updates of the measured errors. This approach is valid areas characterized by simple geology but may fail in complex environments.

In this paper, we propose a new methodology for constructing image perturbations based on the time-lag extended imaging condition and focusing analysis. We demonstrate that the image perturbation can be easily calculated by a simple multiplication of image derivatives and measured focusing errors. We also demonstrate that this type of image perturbation is fully consistent with the linearization embedded in WEMVA. We illustrate our method by applying the technique to the complex Sigsbee 2A model.

Theory

In this section, we summarize the MVA technique described in greater detail by Yang and Sava (2009). Under the single scattering approximation, seismic migration consists of two steps: wavefield reconstruction followed by the application of an imaging condition. Wavefield reconstruction involves constructing solutions to a wave-equation with recoreded data as initial and boundary condition. The reconstructed source and receiver wavefields are kinematically equivalent at discontinuities, and can be represented as four-dimensional objects function of position $\mathbf{x} = (x, y, z)$ and frequency ω,

$$u_s = u_s(\mathbf{x}, \omega) \ , \tag{1}$$

$$u_r = u_r(\mathbf{x}, \omega) \ . \tag{2}$$

Any mismatch between the wavefields indicates inaccurate wavefield reconstruction typically assumed to be due to inaccurate velocity. An imaging condition is designed to extract from these extrapolated wavefields the locations where reflectors occur in subsurface. A conventional imaging condition (Claerbout,

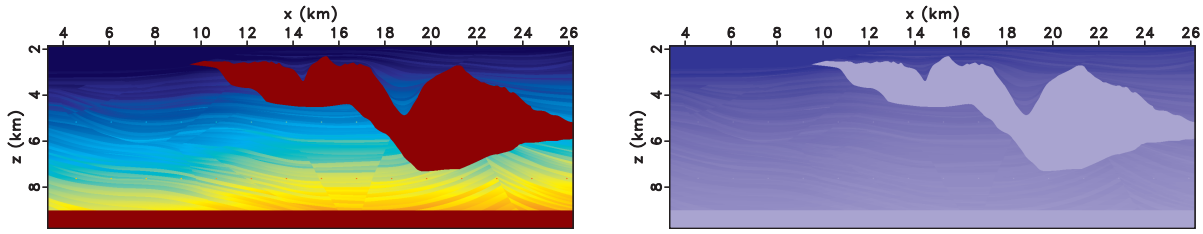

(a) (b)

Figure 1: (a) Sigsbee 2A synthetic model and (b) true slowness perturbation

1985) forms an image as the zero cross-correlation lag between the source and receiver wavefields:

$$r(\mathbf{x}) = \sum_{\omega} u_r(\mathbf{x},\omega)\, u_s^*(\mathbf{x},\omega) \ , \tag{3}$$

where r is the image of subsurface and * represents complex conjugation. An extended imaging condition (Sava and Fomel, 2006) extracts the image by cross-correlation between the wavefields shifted by the time-lag τ:

$$r(\mathbf{x},\tau) = \sum_{\omega} u_r(\mathbf{x},\omega)\, u_s^*(\mathbf{x},\omega)\, e^{2i\omega\tau} \ . \tag{4}$$

Other types of extensions include space-lags or reflection angles (Sava and Fomel, 2003).

When the model used for imaging is erroneous, the images are formed incorrectly. This incorrect imaging is equivalent to a shift of focusing from zero to nonzero time-lags (Yang and Sava, 2008). Therefore, we can measure the difference between the time-lag at which the reflection focus and the zero axis and define it as the quantity $\Delta\tau$, which we label as time-lag perturbation to be exploited for MVA. Furthermore, we can generalize the WEMVA operators constructed for conventional imaging condition (Sava and Vlad, 2008) to include this type of image extension.

Assume that the slowness perturbation Δs and image perturbation Δr are small, then they can be linearly related by the WEMVA operator $\mathbf{L}$:

$$\Delta r = \mathbf{L}\Delta s \ . \tag{5}$$

Since the information of $\Delta\tau$ is available from measurements performed on time-lag extended images, we can construct image perturbation by a linearization of the image relative to the time-lag parameter:

$$\Delta r(\mathbf{x},\tau) = \frac{\partial r(\mathbf{x},\tau)}{\partial \tau}\Delta\tau, \tag{6}$$

where the extended image derivative with respect to time-lag τ is

$$\frac{\partial r(\mathbf{x},\tau)}{\partial \tau} = \sum_{\omega} (2i\omega)\, u_r(\mathbf{x},\omega)\, u_s^*(\mathbf{x},\omega)\, e^{2i\omega\tau}. \tag{7}$$

Notice that the construction of the extended image derivative requires the same procedure as the one used for constructing the extended images. The additional term $2i\omega$ acts as a scaling factor applied at each frequency. As discussed by Yang and Sava (2009), this image perturbation is consistent with the linearized image perturbations required by the WEMVA operator.

Example

We illustrate our methodology using the Sigsbee 2A model (Paffenholz et al., 2002). We use a scaled version of the true model as the background slowness model for migration with extended images. We refer to the difference between the true and background slowness models as the true slowness perturbation Δs. Figure 1(a) and 1(b) shows the velocity profile of the model and true slowness perturbation respectively.

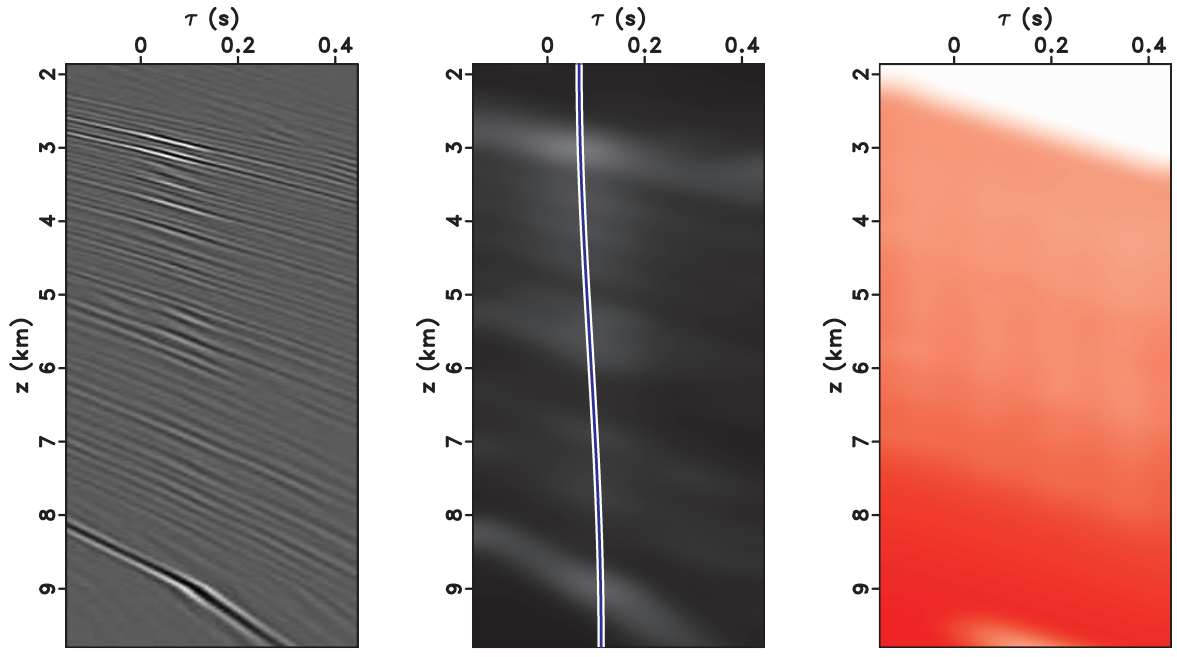

(a) (b) (c)

Figure 2: (a) Time-lag CIG panel. (b) Time-lag CIG panel after the envelope operation, with the picking result overlain. (c) Constructed time-lag perturbation panel.

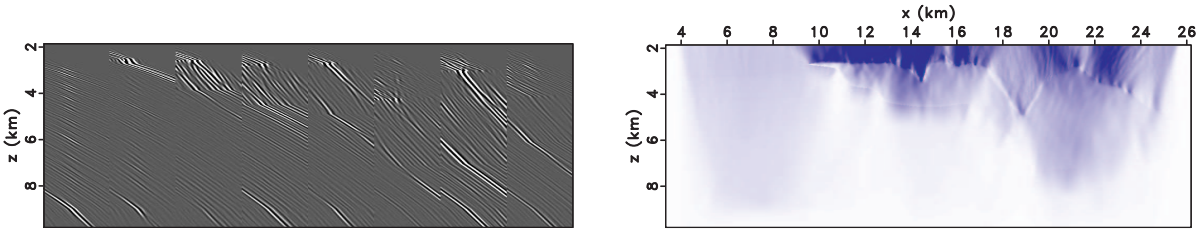

(a) (b)

Figure 3: (a) Image perturbation obtained by the linearized extended image procedure. (b) Slowness perturbation obtained by applying the adjoint WEMVA operator to image perturbation (b).

Figure 2(a) to 2(c) illustrate the procedure of constructing $\Delta\tau$ panel. Figure 2(a) shows a time-lag CIG panel on which we need to pick $\Delta\tau$. To obtain a more accurate picking, we first apply an envelope operation to improve the focusing of the events in the panel, as shown in Figure 2(b). Next, we spread the time-lag perturbation evenly along the events from top to bottom and obtain the $\Delta\tau$ panel, as shown in Figure 2(c).

Figure 3(a) depicts the image perturbation constructed by the procedure discussed in the preceding section. Figure 3(b) depicts the slowness perturbation back-projected from the constructed image perturbation stacked for all shots, which is the result of applying the adjoint WEMVA operator. The back-projection shows that the consistence between the illumination pattern and the illumination of the corresponding migration procedure.

This example demonstrates that our procedure is applicable to a shot-record imaging framework in complex media. This conclusion makes our technique particularly attractive for MVA using wide-azimuth data. However, there is no particular limitation of the type of carrier used to transfer the time-lag information measured on the migrated images into velocity updates. We could, in principle, use plane waves instead of shots as information carrier, thus achieving even higher computational efficiency.

Conclusions

We develop a new method to construct image perturbations for wave-equation migration velocity analysis. The methodology relies on the focusing information extracted from time-lag extended images. The shift of the reflection focusing along the time-lag axis provides a measure of error. We use this information in conjunction with image derivatives relative to the time-lag parameter to construct image perturbations. Compared with more conventional techniques for constructing image perturbations, our approach is efficient, since it represents a relatively trivial extension of the time-lag extended imaging condition, and accurate, since it does not make use of Stolt-like procedures which incorporate strong assumptions about the smoothness of the background model. The results obtained using the complex Sigsbee 2A model demonstrate the validity of our method in complex environments.

Acknowledgments

We acknowledge the support of the sponsors of the Center for Wave Phenomena at Colorado School of Mines. This work is also partially supported by a research grant from StatoilHydro.

REFERENCES

Albertin, U., P. Sava, J. Etgen, and M. Maharramov, 2006, Image differencing and focusing in wave-equation velocity analysis: Presented at the 68th Mtg., Abstracts, Eur. Assoc. Expl. Geophys.

Claerbout, J. F., 1985, Imaging the Earth's interior: Blackwell Scientific Publications.

Higginbotham, J. H., and M. P. Brown, 2008, Wave equation migration velocity focusing analysis: Presented at the 78th Annual International Meeting, SEG, Expanded Abstracts.

Paffenholz, J., B. McLain, J. Zaske, and P. Keliher, 2002, Subsalt multiple attenuation and imaging: Observations from the sigsbee 2b synthetic dataset: 72nd Annual International Meeting, SEG, Expanded Abstracts, 2122–2125.

Pratt, R. G., 1999, Seismic waveform inversion in the frequency domain, Part 1: Theory and verification in a physical scale model: Geophysics, **64**, 888–901.

Sava, P., 2003, Prestack residual migration in the frequency domain: Geophysics, **67**, 634–640.

Sava, P., and B. Biondi, 2004a, Wave-equation migration velocity analysis - I: Theory: Geophysical Prospecting, **52**, 593–606.

———, 2004b, Wave-equation migration velocity analysis - II: Subsalt imaging examples: Geophysical Prospecting, **52**, 607–623.

Sava, P., and S. Fomel, 2003, Angle-domain common image gathers by wavefield continuation methods: Geophysics, **68**, 1065–1074.

———, 2006, Time-shift imaging condition in seismic migration: Geophysics, **71**, S209–S217.

Sava, P., and I. Vlad, 2008, Numeric implementation of wave-equation migration velocity analysis operators: Geophysics, **73**, VE145–VE159.

Sirgue, L., and R. Pratt, 2004, Efficient waveform inversion and imaging: A strategy for selecting temporal frequencies: Geophysics, **69**, 231–248.

Woodward, M. J., 1992, Wave-equation tomography: Geophysics, **57**, 15–26.

Yang, T., and P. Sava, 2008, Wave-equation extended images applied to semblance and depth focusing velocity analysis: 78th Annual International Meeting, SEG, Expanded Abstracts, 2351–2354.

———, 2009, Wave-equation migration velocity analysis using extended images: Presented at the 79th Annual International Meeting, SEG, Expanded abstracts.